JOURNAL OF GEOPHYSICAL RESEARCH, VOL. 107, NO. A6, 1075, 10.1029/2001JA000109, 2002

Hill model of transpolar potential saturation: Comparisons with MHD simulations

G. L. Siscoe and G. M. Erickson
Center for Space Physics, Boston University, Boston, Massachusetts, USA

B. U. Ö. Sonnerup
Thayer School of Engineering, Dartmouth College, Hanover, New Hampshire, USA

N. C. Maynard, J. A. Schoendorf, K. D. Siebert, D. R. Weimer, W. W. White, and G. R. Wilson
Mission Research Corporation, Nashua, New Hampshire, USA

Received 17 April 2001; revised 17 September 2001; accepted 28 September 2001; published 12 June 2002.

[1] We present a comparison between a simple but general model of solar wind-magnetosphere-ionosphere coupling (the Hill model) and the output of a global magnetospheric MHD code, the Integrated Space Weather Prediction Model (ISM). The Hill model predicts transpolar potential and region 1 currents from environmental conditions specified at both boundaries of the magnetosphere: at the solar wind boundary, electric field strength, ram pressure, and interplanetary magnetic field direction; at the ionospheric boundary, conductance and dipole strength. As its defining feature, the Hill model predicts saturation of the transpolar potential for high electric field intensities in the solar wind, which accords with observations. The model predicts how saturation depends on boundary conditions. We compare the output from ISM runs against these predictions. The agreement is quite good for non-storm conditions (differences less than 10%) and still good for storm conditions (differences up to 20%). The comparison demonstrates that global MHD codes (like ISM) can also exhibit saturation of transpolar potential for high electric field intensities in the solar wind. We use both models to explore how the strength of solar wind-magnetosphere-ionosphere coupling depends on the strength of Earth's magnetic dipole, which varies on short geological timescales. As measured by power into the ionosphere, these models suggest that magnetic storms might be considerably more active for high dipole strengths. *INDEX TERMS:* 2736 Magnetospheric Physics: Magnetosphere/ionosphere interactions; 2748 Magnetospheric Physics: Solar wind/magnetosphere interactions; 2760 Magnetospheric Physics: Plasma convection; 2753 Magnetospheric Physics: Numerical modeling; *KEYWORDS:* Transpolar Potential, Polar Cap Potential, Saturation

1. Solar Wind–Magnetosphere–Ionosphere Coupling

[2] Total region 1 current, I_1, and transpolar potential, Φ_{pc}, epitomize solar wind-magnetosphere-ionosphere (SW-M-I) coupling. Progress in understanding this subject can almost be measured by how well the field predicts these quantities. (Region 2 currents, which this paper does not treat, are also an important aspect of the story. In section 7 we discuss how they might affect results presented here.) First models of SW-M-I coupling, reviewed by *Reiff and Luhmann* [1986], assumed one-way coupling from the solar wind to the ionosphere in which magnetic reconnection at the magnetopause taps a fraction of the solar wind potential across the magnetosphere, Φ_{sw}, to yield an available magnetospheric convection potential Φ_m. Φ_m is then impressed via equipotential magnetic field lines onto the ionosphere, where it becomes the Φ_{pc} that generates region 1 currents. The envisioned process was therefore linear. Empirical formulas based on this linear assumption work fairly well, except they tend to overpredict Φ_{pc} for big values of Φ_{sw}. This tendency has been called saturation of the transpolar potential at high values [*Reiff and Luhmann*, 1986; *Russell et al.*, 2000].

[3] *Hill et al.* [1976] presented a model of SW-M-I coupling that manifests saturation intrinsically and at about the observed value. (*Hill* [1984] developed the implications of the model further. We therefore refer to it as the Hill model.) Saturation is a nonlinear process that, in the Hill model, results from a feedback in which the magnetic field generated by region 1 currents becomes comparable to and opposes the Earth's dipole field at the magnetopause where reconnection occurs. By significantly weakening the field that is reconnecting, I_1 ultimately limits how fast reconnection occurs. The result is that at high potentials the iono-

0148-0227/02/2001JA000109$09.00

sphere controls the convection potential, whereas at low potentials, global reconnection at the magnetopause dominates. Hill's model also predicts that for fixed solar wind conditions, as ionospheric conductance varies, the resulting variations in I_1 and Φ_{pc} exhibit a linear current-voltage relation that is formally the same as the current-voltage relation for a generator with an internal resistance driving an external resistance.

[4] *Fedder and Lyon* [1987] showed that numerical simulation of the SW-M-I system gives a linear current-voltage relation, as the Hill model predicts. Their simulation revealed changes in streamlines of magnetospheric convection that occur as region 1 current increases, leading to saturation. They concur with Hill that at least at high values the ionosphere plays a significant role in regulating convection potential. The Fedder and Lyon work is the first to discuss the role of the ionosphere in controlling magnetospheric convection.

[5] Here we use the Integrated Space Weather Prediction Model (ISM) to further test the Hill model. Like the Fedder and Lyon simulation the ISM simulation substantiates the model's basic conclusions (saturation and linear current-voltage relation). We extend prior work by giving explicit formulas based on the model and ISM simulations that show how, for fixed interplanetary magnetic field (IMF) clock angle, I_1 and Φ_{pc} scale with solar wind electric field, solar wind ram pressure, and the strength of Earth's dipole.

2. Hill SW-M-I Coupling Model

[6] Let Φ_S be the potential across the polar cap that generates region 1 currents whose magnetic field significantly weakens the magnetic field at the magnetopause where reconnection occurs. (The amount of weakening is defined later.) The Hill model postulates that when the available magnetospheric convection potential Φ_m is less than the saturation potentialΦ_S, the transpolar potential Φ_{pc} is approximately Φ_m. However, in the opposite situation, when the available magnetospheric convection potential Φ_m is greater than the saturation potential, the transpolar potential is approximately Φ_S. The Hill model combines these limits in the following expression applicable to all Φ_m:

$$\Phi_{pc}=\Phi_m\Phi_S/(\Phi_m+\Phi_S). \tag{1}$$

Saturation at the value Φ_S automatically results when $\Phi_m \gg \Phi_S$. In the other extreme, Φ_S drops out of the relation, and Φ_{pc} varies linearly with Φ_m. At the transitional value $\Phi_m = \Phi_S$ the transpolar potential is half the available magnetospheric convection potential.

[7] To derive from (1) the linear current-voltage relation applicable to a generator with internal resistance driving an external resistance, introduce the ionospheric Ohm's law in the form

$$I_1 = \xi\,\Sigma\,\Phi_{pc}, \tag{2}$$

where Σ is ionospheric (Pedersen) conductance (assumed, for simplicity, to be uniform) and ξ is a coefficient that depends on the geometry of the currents flowing in the ionosphere. (We will see that it has a value between 3 and 4. It varies systematically with Σ.) In particular,

$$I_S = \xi\,\Sigma\,\Phi_S \tag{3}$$

gives the value of I_1 that significantly weakens the magnetic field at the magnetopause where reconnection occurs. From (2) and (3) we have $\Phi_S = \Phi_{pc}I_S/I_1$, which when substituted into (1) and rearranged gives the desired relation

$$\Phi_{pc} = \Phi_m - (\Phi_m/I_S)I_1. \tag{4}$$

The value Φ_m/I_S is the effective internal resistance of the generator. Note that this is just a formal equivalence. It does not mean that Φ_m/I_S corresponds to a real resistance. Instead, it means that Φ_m/I_S, as the coefficient of I_1, quantifies the internal resistance-like effect that the region 1 circuit mimics by regulating the amount of Φ_m that is imposed across the ionosphere as Φ_{pc}.

[8] The task now is to obtain expressions for Φ_m and I_S to reveal explicitly the Φ_{pc} dependence on solar wind ram pressure, IMF strength and direction, and dipole strength. This will allow us to compare the Hill model quantitatively with the output of ISM runs. It also provides a useful general formula for predicting Φ_{pc} over a wide range of values for these quantities.

3. Expressions for Φ_m, I_S, and Φ_{pc}

[9] We represent the reconnection potential at the magnetopause by

$$\Phi_m \cong \chi\,L_{r0}\,R_E\,E_{sw}\,p_{sw}^{-1/6}\,D^{1/3}\,F(\theta), \tag{5}$$

where L_{r0} is the effective length of the reconnection line in units of Earth radii, R_E (6370 km). E_{sw} is intensity of the motional electric field in the solar wind ($V_{sw}\,B_{sw}$, where *sw* indicates solar wind quantities, V is velocity, and B is magnetic field strength ignoring the component parallel to the wind). Variable p_{sw} is solar wind ram pressure ($\rho_{sw}\,V_{sw}^2$, where ρ_{sw} is solar wind mass density). D is dipole strength normalized to the present value. $F(\theta)$ represents the IMF clock angle dependence of magnetopause reconnection ($F(0) = 0$, $F(\pi) = 1$). In between $\theta = 0$ and $\theta = \pi$ there are several expressions for $F(\theta)$ that have been proposed [*Reiff and Luhmann*, 1986]. The coefficient χ quantifies the effects of magnetosheath compression and reconnection efficiency:

$$\chi = 4\,f_r(2\,\kappa\,\rho_{sw}/\rho_{sh})^{1/2}, \tag{6}$$

where f_r is the reconnection efficiency factor (ratio of reconnection velocity to Alfvén velocity) and ρ_{sh} is the mass density in the magnetosheath. The coefficient κ is the ratio of the stagnation pressure to solar wind ram pressure, which depends on solar wind Mach number according to a well-known expression in aerodynamics [*Spreiter et al.*, 1966]. It is of order unity, and for high Mach numbers it is close to 0.88. The relation ρ_{sw}/ρ_{sh} is found for the Mach number-dependent shock jump relations. (We evaluate the ratio using the aerodynamic shock jump relations and the

magnetosonic Mach number [*Spreiter et al.*, 1966].) To derive the expression for χ we use the *Crooker et al.* [1982] empirical relation for magnetic field strength in the magnetosheath at the magnetopause:

$$B_{sh} \cong 2(B_{sw}\, B_{st})^{1/2}, \tag{7}$$

where B_{st} is the magnetic field strength that balances solar wind stagnation pressure.

[10] Except for this last, purely empirical expression, the terms in (5) and (6) are based on explicit and accepted physics of magnetopause reconnection. The $p_{sw}^{-1/6}D^{1/3}$ factor in (5) comes from Chapman-Ferraro scaling [e.g., *Siscoe*, 1979; *Vasyliunas et al.*, 1982]. The reconnection process is represented by the factor $f_r\ L_{r0}\ F(\theta)$. Values commonly taken for f_r and L_{r0} are 0.1 and 30, respectively (the characteristic width of the magnetosphere at the terminator plane). One therefore expects a priori that the value of the product $f_r\ L_{r0}$ would be ~3.0. We find (see below) that the value 3.3 fits ISM output almost exactly. We therefore adopt this particular (but unexceptional) value for $f_r\ L_{r0}$.

[11] Combining now these various pieces, we evaluate (5) using the magnetosonic Mach number corresponding to the ISM runs discussed below (M_{ms} = 3.74) (results are insensitive to M_{ms} over its most commonly observed range of values):

$$\Phi_m(\mathrm{kV}) = 57.6\ E_{sw}\left(\mathrm{mV\ m^{-1}}\right) p_{sw}\ (\mathrm{nPa})^{-1/6} D^{1/3}\ \mathrm{F}(\theta). \tag{8}$$

[12] To obtain an expression for I_S, we use an idealized geometrical model for the region 1 current system: two circular current loops (for the north and south current systems) that form a figure eight in the terminator plane. (We acknowledge that there are two schools of thought regarding where region 1 currents close in the magnetosphere: through the tail current sheet or across the magnetopause leeward of the dayside cusp. In MHD simulations, however, region 1 currents close over the magnetopause leeward of the cusps [*Tanaka*, 1995, 2000; *Janhunen et al.*, 1996; *Siscoe et al.*, 2000]. We idealize the result by putting the north and south region 1 current systems in the terminator plane.) This current pair generates a southward field at the stagnation point, the strength of which can be written as

$$B_{1s} = G\left(x_{s0,}\ r_{10}\right)\ \mu_0\, I_1 / R_E\, p_{sw}^{1/6}\ D^{-1/3}, \tag{9}$$

where x_{s0} is a characteristic distance (normalized to units of R_E) from the center of the Earth to the stagnation point. (We take x_{s0} = 10.) Variable r_{10} is the corresponding radius of the region 1 current loops. (We take r_{10}/x_{s0} = 3/4, which is consistent with standard magnetospheric shape.) $G(x_{s0}, r_{10})$ is the expression one gets by integrating the Biot-Savart law around a figure eight current loop [*Smythe*, 1950, p. 271]. It scales as inverse distance; hence it has inverse Chapman-Ferraro scaling with respect to (normalized) p_{sw} and D, as the expression shows. Numerically, $G(x_{s0}, r_{10})$ = 0.014. Evaluating terms in (9) gives

$$B_{1s}(\mathrm{nT}) = 2.8\ I_1(\mathrm{MA})\, p_{sw}^{1/6}\ D^{-1/3}. \tag{10}$$

The Hill Ansatz is that $I_S = I_1$ when B_{1s} is a significant fraction, α, of the dipole field at the reconnection site. "Significant fraction," in an unbiased, information-free derivation would be about 1/2. We find (see below) that the value α = 0.41 fits ISM output almost exactly. Accordingly, we adopt this particular (but unsurprising) value. Hill's Ansatz gives the following expression for I_S:

$$I_S = (\alpha/G)(B_0\ R_E)/\left(\mu_0\ x_{s0}^3\right) p_{sw}^{1/3} D^{1/3}, \tag{11}$$

where B_0 is the equatorial, surface strength of the dipole field (3.1×10^{-5} T). The change from (10) to (11) in the pressure-scaling term results from the field strength at the stagnation point scaling as $p_{sw}{}^{1/2}$. Evaluating terms in (11) gives

$$I_s(\mathrm{MA}) = 4.6 p_{sw}^{1/3}\ D^{1/3}. \tag{12}$$

[13] To obtain an expression for Φ_{pc}, we combine (1), (3), (8), and (12):

$$\Phi_{pc}(\mathrm{kV}) = 57.6\ E_{sw} p_{sw}^{1/3}\ D^{4/3}\ F(\theta)/\left(p_{sw}^{1/2}\ D + 0.0125\ \xi\ \Sigma_0\ E_{sw}\ F(\theta)\right), \tag{13}$$

where E_{sw} is in mV m^{-1} and we have introduced the dipole scaling relation for Pedersen conductance [*Rassbach et al.*, 1974]:

$$\Sigma\ =\ \Sigma_0\, D^{-1}. \tag{14}$$

From (13) we see that the saturation value that sets in for high values of E_{sw} is

$$\Phi_S(\mathrm{kV}) = 4610\ p_{sw}^{1/3}\ D^{4/3}/(\xi\ \Sigma_0). \tag{15}$$

Equation (15) reveals important information on how Φ_S depends on environmental conditions. It has no explicit dependence on the IMF clock angle function, $F(\theta)$. $F(\theta)$ is nonetheless present implicitly, for it takes a bigger E_{sw} to reach saturation when $F(\theta)$ is small, that is, for northward IMF. Φ_{pc}(saturation) increases significantly as p_{sw} increases, which might account for its being an elusive quantity to tie down with measurements. The relatively strong dependence on D in (15) arises from the dependence of Pedersen conductance on inverse field strength. For D = 1.5 (which might have been its value 2500 years ago [*McElhinny and Senanyake*, 1982]) the saturation potential increases a factor of 1.7, from a representative storm time value of 250 kV to a never-before-measured 430 kV. Φ_{pc} (saturation) varies inversely with the conductance product $\xi\Sigma$, which means that in saturation mode the magnetosphere acts like a constant current generator with the ionosphere as a resistive load. (One expects this since at saturation, I_1equals I_S, which is a constant.) In the ISM run (discussed below) that represents the actual typical magnetosphere, the $\xi\Sigma$ product is 21.7, which (for D = 1) gives $\Phi_S \cong 212\ p_{sw}^{2/3}$ kV. Since p_{sw} is typically between 1 and 1.5 nPa, Φ_{pc}(saturation) is typically between 200 and 300 kV, which is a range that has been noted in data.

[14] By setting Φ_{pc} given by (13) equal to one half of Φ_S as given by (15), we find the following expression for the value of E_{sw} that divides unsaturated from saturated dependence of Φ_{pc} on Φ_m:

$$E_{sw}(\text{threshold}) = 80\ p^{1/2}\ D/\xi\ \ \Sigma_0\, F(\theta). \tag{16}$$

Note that it takes a bigger E_{sw} to reach saturation when $F(\theta)$ is small, as previously mentioned. Substituting representative values into (16) and setting $F(\theta) = 1$, we find as a typical value for E_{sw} (threshold) $\sim$4 mV m^{-1}.

[15] The current-voltage relation (4) becomes

$$\Phi_{pc}(\text{kV}) = \left(57.6\ E_{sw} p_{sw}^{-1/6}\ D^{1/3} - 12.5\ E_{sw} p_{sw}^{-1/2}\ I_1\right) F(\theta). \tag{17}$$

For later comparison with ISM output we evaluate (17) with $E_{sw} = 1.75$ mV m^{-1}, $p_{sw} = 1$ nPa, $D = 1$, and $\theta = \pi$:

$$\Phi_{pc}(\text{kV}) \cong 101 - 21.8\ I_1(\text{MA}). \tag{18}$$

[16] The constant, 101 kV, is the open-circuit potential of the pseudocircuit. One might have expected it to equal the full solar wind potential across the magnetosphere, which is $\sim$350 kV. The difference between these numbers arises through the coefficient χ in (5) that quantifies the effects of magnetosheath compression and reconnection efficiency. χ is the ratio of the open-circuit potential to the full solar wind potential. Its value, as given by (6) for the canonical parameters used here for illustration, is 0.29.

4. Parametric Exploration of the Hill Model

[17] Equation (13) for Φ_{pc} could be of great utility in magnetospheric physics since it combines in one formula, information describing how the transpolar potential depends on pertinent boundary conditions at both "ends" of the magnetosphere. At the solar wind end it specifies the dependence on motional electric field and ram pressure,

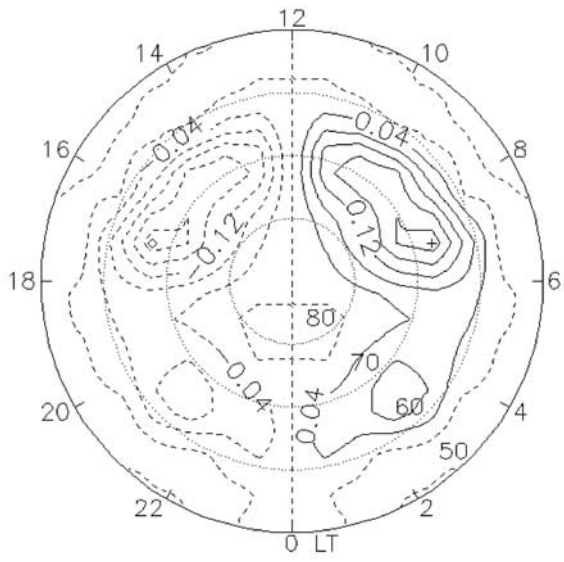

Figure 1. Contours of parallel current (in units of μA m^{-2}).

Table 1. Transpolar Potentials and Region 1 Currents Obtained From Computer Runs With the ISM MHD Code[a]

Σ, S	Φ_{pc}, kV	I_1, MA	ξ
2	87.7	0.74	4.2
6	70.5	1.5	3.6
18	45.7	2.5	3.1
44	28.6	3.5	2.8

[a] ISM, Integrated Space Weather Prediction Model.

and at the ionospheric end it specifies the dependence on ionospheric conductance and dipole strength. The ionospheric conductance term is, however, not completely specified since it enters as the product $\xi\Sigma$ in which ξ depends on the geometry of the ionospheric closure of the currents. For example, in an ideal geometry in which transpolar potential is distributed sinusoidally around a circle in a planar ionosphere with uniform conductance, $\xi = 2$ [*Crooker and Siscoe*, 1981]. Observed region 1 currents, however, are not distributed sinusoidally around the polar cap boundary with peaks in the terminator meridian. Instead, the currents concentrate in the forenoon and afternoon local time quadrants [*Iijima and Potemra*, 1976]. This tendency is seen in Figure 1, which shows parallel currents in the northern polar regions as determined by an ISM simulation for the case $\Sigma = 6$ S. One can readily show that one consequence of shifting the centers of I_1 concentration from the terminator meridian toward noon, as seen in Figure 1, is to increase ξ. As mentioned in section 1, in ISM runs ξ tends to lie between 3 and 4, but it varies systematically with Σ. To render the general formula for Φ_{pc} (13) more useful, therefore, we use ISM outputs to find a numerical relation between ξ and Σ.

[18] Parameters for the ISM runs used in this investigation are the following: solar wind speed is 350 km s^{-1}, solar wind density is 5 protons cm^{-3}, solar wind temperature is 20 eV (protons and electrons), interplanetary magnetic field is 5 nT, the IMF clock angle is π (precisely south), and $D = 1$. (The ISM code is described in detail by *White et al.* [2001].) (Since these are $D = 1$ runs, the conductances correspond to Σ_0 in the notation of (13) and (14). For notational economy we suppress the subscripted zeroes in this section.) In these runs, ionospheric conductance is uniform (except for a small latitudinal variation due to the dependence of conductance on field strength). Runs were made with $\Sigma = 2$, 6, 18, and 44 S. Solar wind and ionospheric boundary conditions are steady in each run. Table 1 gives information from these runs that is pertinent to this investigation.

[19] Below we compare the computed potential and current given in Table 1 with the Hill model. Here we are interested in analytically parameterizing the dependence of ξ on Σ. The expression

$$\xi = 4.45 - 1.08 \log \Sigma \tag{19}$$

fits the values in Table 1 with a correlation coefficient 0.993. This formula substituted into (13) gives an expression for Φ_{pc} in terms only of explicit boundary parameters. Of course, ξ might depend on boundary parameters in addition to Σ; thus (19) is "certified" only for parameters approximately like those chosen as inputs for the ISM runs behind Table 1. We use (19) to explore how according

to (13), Φ_{pc} varies with each of its parameters separately, holding the other parameters fixed. An alternative approach would be to carry out the exploration with a fixed value for ξ (3.4, say, which is the average of the values in Table 1). By using (19), however, we capture what is probably a general tendency of ξ to decrease with Σ, and so it is probably better than using a fixed ξ.

[20] Figure 2 shows how Φ_{pc} varies with E_{sw}. The thick curve labeled "baseline" illustrates the variation for baseline values for the other parameters: $\Sigma = 6$ S, $p_{sw} = 1$ nPa, $\theta = \pi$ (rather $F(\pi) = 1$), and $D = 1$. The plot reveals that saturation sets in somewhat gradually. By $E_{sw} = 50$ mV m^{-1}, Φ_{pc} reaches 198 kV compared to the saturation value of 212 kV. One reaches 90% of saturation (or 191 kV) at $E_{sw} = 33$ mV m^{-1}, which corresponds to an IMF of 33 nT moving at 1000 km s^{-1}. Nonetheless, the effect of the ionosphere to reduce Φ_{pc} relative to Φ_m sets in relatively quickly. For example, Φ_{pc} is less than one-half Φ_m already for $E_{sw} = 4$ mV m^{-1}. As Figure 3 shows, the curve quantitatively resembles a plot of transpolar potential versus interplanetary electric field derived for the storm of 24–25 September 1998 [*Russell et al.*, 2000, p. 1373].

[21] The curve labeled $p_{sw} = 10$ (nPa) illustrates the effect that a factor of 10 increase in solar wind ram pressure has on elevating the saturation value of Φ_{pc}. It also illustrates that the saturation value is probably never reached for very high ram pressures. Value Φ_{pc} is nonetheless significantly suppressed relative to Φ_m.

[22] The curve labeled $\Sigma = 12$ (S) illustrates that increasing ionospheric conductance (in this case from 6 to 12 S) decreases Φ_{pc} at all values of E_{sw}. Here a factor of 2 increase in Σ reduces the saturation value to 55% of the baseline value. Since Σ and p_{sw} tend to increase together during disturbed conditions, the increase in one tends to counter the increase in the other, thereby preserving a baseline-like dependence of Φ_{pc} on E_{sw}. Indeed, the two values chosen here for illustration in Figure 2 ($p_{sw} = 10$ and $\Sigma = 12$) implemented together produce a curve almost identical to the baseline curve.

[23] The curve labeled $\theta = \pi/2$ typifies more usual IMF conditions and so should perhaps be labeled "baseline." To make this curve we have used $F(\theta) = \sin^2(\theta/2)$, which is the simplest of proposed IMF clock angle functions [*Kan and Lee*, 1979]. It illustrates the expected decreases of Φ_{pc} when the IMF clock angle swings northward from the chosen baseline $\theta = \pi$. Relative to the baseline curve, Φ_{pc} is less at all values of E_{sw}, but it approaches the same saturation value, just more slowly. Interestingly, the change from $\theta = \pi$ to $\theta = \pi/2$ has a smaller effect on reducing Φ_{pc} than has the ionospheric feedback effect as quantified by the difference between Φ_{pc} and Φ_m.

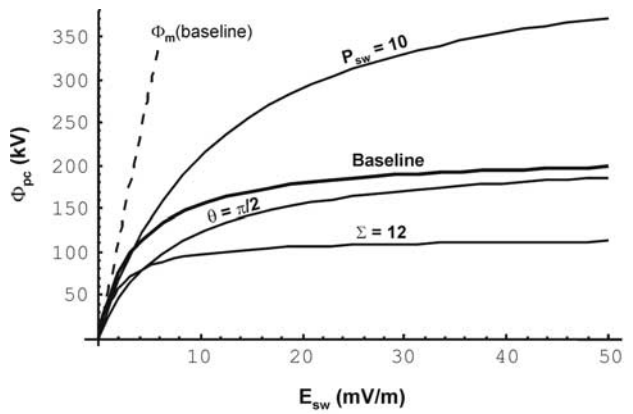

Figure 2. Variation of Φ_{pc} with E_{sw} for different departures of boundary parameters from baseline values, as indicated. The baseline values are $p_{sw} = 1$ nPa, $\Sigma = 6$ S, $\theta = \pi$, and $D = 1$. Variable Φ_m is the magnetopause reconnection potential.

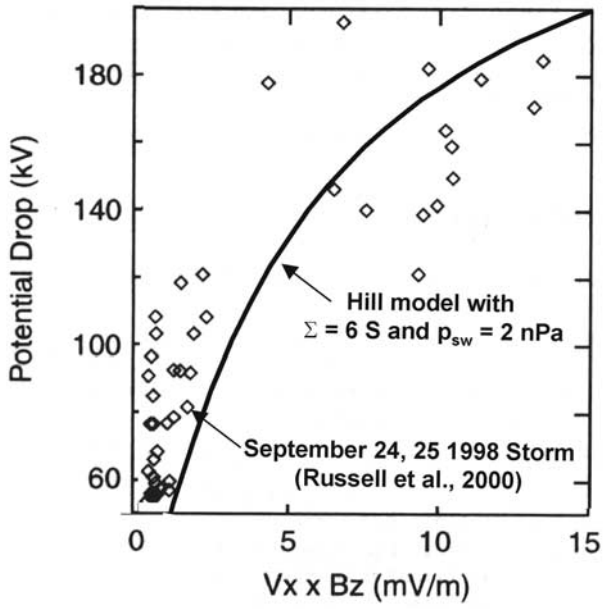

Figure 3. Comparison of saturation as given by Hill model and as revealed in data from a magnetic storm as analyzed by *Russell et al.* [2000].

5. Comparison With ISM Runs

[24] We examine next how well ISM outputs as presented in Table 1 support or otherwise the Hill model. Figure 4 gives a plot of the computed current-voltage relation

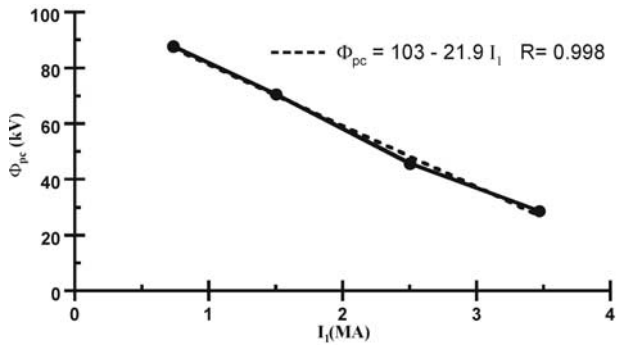

Figure 4. The current-voltage relation generated by the Integrated Space Weather Prediction Model (ISM) code and a linear fit to it.

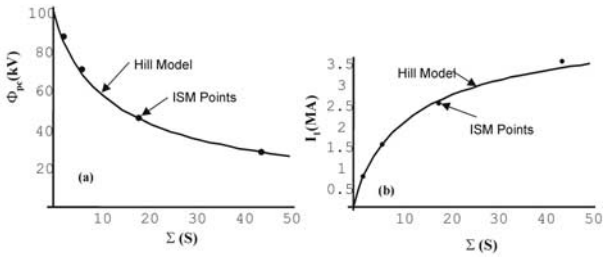

Figure 5. (a) A comparison of Φ_{pc} versus Σ as determined with the Hill model and with the ISM. (b) A comparison of I_1 versus Σ as determined with the Hill model and with the ISM.

(Table 1). The relation is very closely linear, as found also for the simulations that *Fedder and Lyon* [1987] examined. This behavior is characteristic of the I–V curve of a generator with internal resistance driving an external resistance as predicted by the Hill model. The linear fit to the curve is

$$\Phi_{pc}(\mathrm{kV}) = 103 - 21.9\, I_1\ (\mathrm{MA}), \tag{20}$$

which corresponds to an "internal resistance" of 0.022 Ω. This result is very similar to (17) above that was obtained for the Hill model. It is true that (17) was "tuned" with this ultimate comparison in mind, but the tuning was fine not coarse. This current-voltage relation is independent of conductance product $\xi\Sigma$, which is the parameter that is eliminated between the ionospheric Ohm's law and the expression for I_S to arrive at (17) from the Hill equation (1). Thus it is free from uncertainty due to variability of the value of ξ.

[25] Figure 5 gives another way to compare the Hill model with results of ISM runs. The curves for Φ_{pc} and I_1 are obtained from (13) and (2), respectively, with (18) used to evaluate ξ. Other parameters are "baseline" (E_{sw} = 1.75 mV m^{-1}, p_{sw} = 1 nPa, D = 1, and $\theta = \pi$). The points are ISM values listed in Table 1. Again, the agreement is quite good. Evidently, the ISM code simulates the physics of the Hill model over the range of parameters compared.

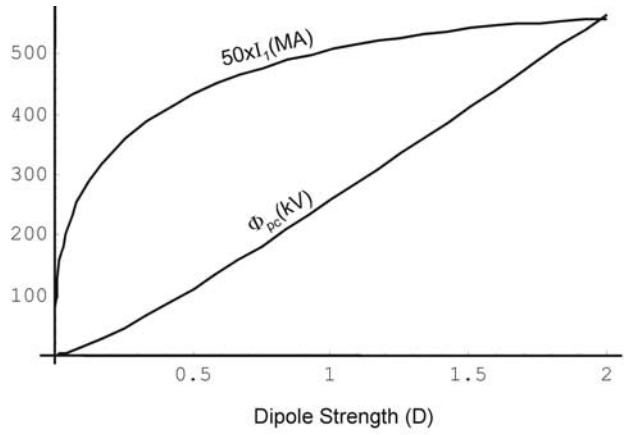

Figure 6. Variation of Φ_{pc} and I_1 with dipole strength for storm (Bastille Day) conditions.

6. SW-M-I Coupling as a Function of Dipole Strength

[26] We live at a time when the strength of the geomagnetic dipole is decreasing rapidly on a geological timescale. By setting D = 0.5 in (13) and (2) the Hill model allows us to estimate the strength of SW-M-I coupling under conditions toward which the Earth might be heading and which typify the average dipole strength over the last Ice Age [*Merrill et al.*, 1998, p. 129]. Archeomagnetic data, on the other hand, indicate that the dipole has been stronger than at present for more than 4000 years. It passed through a broad maximum in strength that crested a little less than 3000 years ago when it approached 1.5 times the present value [*McElhinny and Senanyake*, 1982]. Setting D = 1.5 therefore allows us to estimate the strength of SW-M-I coupling at times corresponding to the mythopoetic and classical ages of Greece, Egypt, and Mesopotamia. To make the comparison interesting, we explore dipole strength dependence of the model under storm time conditions: E_{sw} = 50 mV m^{-1}, Σ = 12 S, p_{sw} = 16.7 nPa, and $\theta = \pi$. These parameters represent conditions during the so-called Bastille-Day storm of 2000.

[27] Figure 6 shows how, according to (3), (13), and (18) with ξ set to a constant 3.5, Φ_{pc} and I_1 vary as a function of dipole strength under Bastille Day conditions. Perhaps unsurprisingly, current and potential increase monotonically with D. What is perhaps surprising, however, is the big range of variation in Φ_{pc}. It is 103, 243, and 391 kV for D = 0.5, 1.0, and 1.5, respectively. Current varies less: 8.7, 10.2, and 10.9 MA, in the same order. The power into the ionosphere is approximately the product of these two quantities: 0.9, 2.5, and 4.3 TW, respectively. As inferred on the basis of input power to the ionosphere (other things being equal), storms might have been considerably more active between 2000 and 3000 years ago than now. Earlier than 15,000 years ago, storms might have been relative dull affairs compared to the present, and they might become so again in the (geologically) near future.

[28] We have run ISM under Bastille Day conditions for D = 0.5, 1, and 1.5. The results compared with the Hill model are given in Table 2. The Hill values in this case are based on the values of ξ given in Table 2 (instead of the average value 3.5) for closer comparison. The ISM values show the same strong dependence of Φ_{pc} on D as the Hill model values and the same relatively flat dependence of I_1 on D, although direct comparison with Figure 6 is prevented by Σ_o being different for each run. The two sets of numbers generally agree within 10–20%. The

Table 2. Comparison Between Values of Transpolar Potentials and Region 1 Currents Obtained by ISM and the Hill Model for Three Different Dipole Strengths[a]

D	Σ_o	ξ	Φ_{pc} (ISM)	Φ_{pc} (Hill)	I_1 (ISM)	I_1 (Hill)
0.5	12	2.9	135	123	9.5	8.6
1.0	12	4.0	243	216	11.7	10.4
1.5	12	3.6	455	382	13.2	11.0

[a] The ionospheric conductance varies between runs as shown (scaled by equation (14) to equivalent conductances for D = 1). Conductances are in siemens, potentials are in kilovolts, and currents are in megamperes.

differences between the two sets of potentials for a fixed D are much less than the change in the potentials between successive values of D. ISM potentials are bigger than Hill model potentials, which might reflect an inaccuracy in Chapman-Ferraro (C–F) scaling for size ($p^{-1/6}D^{1/3}$) when (as for Bastille Day conditions) the IMF is strong and southward. Then the magnetosphere is wider than C–F scaling predicts, which would increase the potential. In any case the agreement between the numbers, which compares a relatively simple model with a full-up global MHD simulation in a parameter regime never before explored, is impressive.

[29] Looking at the result from the opposite direction, we may infer that since the ISM results obey the predictions of the Hill model to a good-to-excellent approximation, MHD simulations, as represented by ISM, must exhibit the defining feature of the Hill model, that is, saturation of the transpolar potential. We can demonstrate this property directly by comparing the baseline case (unsaturated) against the Bastille Day case (saturated) with respect to the fraction of solar wind potential Φ_{sw} that is impressed across the polar cap as Φ_{pc}. For this we take Φ_{sw} to be given by the following expression:

$$\Phi_{sw} = E_{sw} L_{r0} R_E p^{-1/6} D^{1/3}. \quad (21)$$

Then the baseline ratio (from Table 1) is $\Phi_{pc}/\Phi_{sw} = 70.5/368 = 0.19$, whereas the Bastille Day ratio (from Table 2, $D = 1$) is $243/6570 = 0.037$. The magnetosphere's capture efficiency for solar wind potential drops from 19% for unsaturated baseline conditions to 3.7% for saturated Bastille Day conditions. This example illustrates how poorly a linear extrapolation of Φ_m to high values approximates Φ_{pc}. For Bastille Day conditions and $D = 1$, Φ_m is 1800 kV versus 243 kV for Φ_{pc} according to ISM. As the comparison in Table 2 demonstrates, the Hill model gives a value in much better agreement with MHD simulations (in this case, 216 kV versus 243 kV).

[30] A discussion of the origin of saturation in an MHD code is different than that given above in connection with the Hill model with its emphasis on the feedback from region 1 current. *Raeder et al.* [2002] have shown that in an MHD code, saturation results as follows. As the solar wind electric field becomes more geoeffective, the magnetopause develops "shoulders" poleward of the cusps that choke the flow into the reconnection site at low latitudes. Of course, the two modes of description are mutually consistent (region 1 currents are "responsible" for the shoulders), but they emphasize different aspects of the phenomenon.

7. Effects of Region 2 Currents

[31] The Hill model as presently formulated ignores region 2 currents. MHD simulations of SW-M-I coupling generally produce weak region 2 currents. (A discussion of the reason for this property goes beyond what is appropriate here. It has to do with particle-drift physics rather than MHD physics dominating the inner magnetosphere where region 2 currents arise.) In a sense, the comparison between the Hill model and ISM results has been facilitated by the property of MHD codes to produce weak region 2 currents. We know enough about region 2 currents both empirically and theoretically, however, to evaluate how they might affect results presented here were they to be included. Two effects in particular stand out as being potentially significant. Region 2 currents might modify the expression for the saturation current I_S, and they will likely change the value of ξ in the whole-ionosphere Ohm's law (equation (2)).

[32] Region 2 currents will affect the value of I_S if, compared to region 1 currents, they generate a significant magnetic field at the site of magnetopause reconnection. Then, since region 2 currents circulate in a sense opposite to region 1 currents, I_S would have to be increased. It is probably the case, however, that compared to region 1 currents, region 2 currents generate a substantially weaker magnetic field at the site of magnetopause reconnection. This seems likely because whereas region 1 currents close (according to MHD simulations) high over the magnetopause, and so are well distributed to produce a significant field at the dayside magnetopause, region 2 currents close low and behind the Earth as a partial ring current [e.g., *Erickson et al.*, 1991]. The site of dayside magnetopause reconnection therefore lies farther from the region 2 current system and in its weak-field latitude zone. We can estimate the relative contributions that the two current systems make to the magnetic field at the stagnation point (representing the site of magnetopause reconnection) using wire loop models. Earlier, we used a figure eight wire loop model to estimate the strength of the region 1 current system at the stagnation point. At a similar level of sophistication, we can represent the region 2 current system by a circular wire loop lying in the equatorial plane touching the Earth and the inner edge of the plasma sheet tangentially. Then, taking the radius of this loop to be 5 R_E, we find, for the typical case $I_2 = 0.75I_1$ [*Iijima and Potemra*, 1976], that its field at the stagnation point is 22% as strong as the field from the region 1 current system. The impact on the present calculation, were we to pursue it, would be to increase the effective value of α in (11) from 0.41 to 0.53.

[33] The second effect that region 2 currents will have on the current-voltage relation is to increase the value of ξ in the whole-ionosphere Ohm's law (equation (2)) [*Crooker and Siscoe*, 1981]. Depending on geometry, the increase can be big (a factor of 2–4 if the current systems are close together so that it is easier for region 1 currents to close through the region 2 system than through the ionosphere) or small (less than a factor of 2 if the currents are well separated). Evidently, the increase is not big. We infer this from typical measured values of the transpolar potential (60 kV) and region 1 currents (2 MA). The current-to-voltage ratio of these typical values is 33. For the baseline (i.e., typical) ISM run, which displays weak region 2 currents, the ratio (from Table 1) is 21. There does not seem to be enough room between this approximately region 2-less ratio and the ratio that nature exhibits for a factor of 2 or more increase owing to region 2 currents. In any case, whatever its value, the increase can be readily accommodated within the Hill model by adjusting ξ. It will have the same effect as an increase in conductance in Figures 1 and 3, that is, to decrease the transpolar potential, to increase the region 1 currents, and to decrease the saturation potential.

8. Summary: An Assessment of the Hill Model

[34] The Hill model is perhaps the simplest model that builds saturation automatically into an expression for the transpolar potential. It gives a basic principle for formulating the term that leads to saturation. As formulated here, it relates the transpolar potential to external and internal boundary conditions (solar wind motional electric field and ram pressure, IMF direction, ionospheric conductance and current closure pattern, and dipole strength). For typical non-storm conditions (''baseline'') a comparison between transpolar potential and region 1 currents obtained with the Hill model and with the ISM MHD simulation code shows good agreement. The current-voltage relations obtained by varying ionospheric conductance while holding other boundary conditions fixed are nearly identical between the Hill and MHD models when the Hill model is tuned (slightly) to maximize the agreement. Comparisons for storm conditions (the Bastille Day runs) and for different dipole strengths also show good agreement. They show that the Hill model is much better than the magnetopause reconnection voltage for estimating the transpolar potential for high values of the solar wind electric field (i.e., for storm conditions).

[35] **Acknowledgments.** This work was supported in part by the NSF under grant ATM98-12678 and NASA under grants NAG5-8135 and NASW-99014. Development of the ISM code was supported by the Defense Threat Reduction Agency, 45045 Aviation Drive, Dulles, VA 20166-7517.

[36] Janet G. Luhmann thanks Takahashi Tanaka and another referee for their assistance in evaluating this paper.

References

Crooker, N. U., and G. L. Siscoe, Birkeland currents as the cause of the low- latitude asymmetric disturbance field, *J. Geophys. Res.*, *86*, 11,201–11,210, 1981.

Crooker, N. U., G. L. Siscoe, P. R. Mullen, C. T. Russell, and E. J. Smith, Magnetic field compression at the dayside magnetopause, *J. Geophys. Res.*, *87*, 10,407–10,412, 1982.

Erickson, G. M., R. W. Spiro, and R. A. Wolf, The physics of the Harang discontinuity, *J. Geophys. Res.*, *96*, 1633–1645, 1991.

Fedder, J. A., and J. G. Lyon, The solar wind-magnetosphere-ionosphere current-voltage relationship, *Geophys. Res. Lett.*, *14*, 880–883, 1987.

Hill, T. W., Magnetic coupling between solar wind and magnetosphere: Regulated by ionospheric conductance?, *Eos Trans. AGU*, *65*, 1047, 1984.

Hill, T. W., A. J. Dessler, and R. A. Wolf, Mercury and Mars: The role of ionospheric conductivity in the acceleration of magnetospheric particles, *Geophys. Res. Lett.*, *3*, 429–432, 1976.

Iijima, T., and T. A. Potemra, Field-aligned currents in the dayside cusp observed by Triad, *J. Geophys. Res.*, *81*, 2165–2174, 1976.

Janhunen, P., H. E. J. Koskinen, and T. I. Pulkkinen, A new global ionosphere-magnetosphere coupling simulation utilizing locally varying time step, in *Proceedings of the Third International Conference on Substorms (ICS-3), Eur. Space Agency Spec. Publ., EAS SP-389*, 205–210, 1996.

Kan, J. R., and L. C. Lee, Energy coupling function and solar wind-magnetosphere dynamo, *Geophys. Res. Lett.*, *6*, 577–580, 1979.

McElhinny, M. W., and W. E. Senanyake, Variations in the geomagnetic dipole, 1, The past 50,000 years, *J. Geomagn. Geoelectr.*, *34*, 39–51, 1982.

Merrill, R. T., M. W. McElfinney, and P. L. McFadden, *The Magnetic Field of the Earth*, Academic, San Diego, Calif., 1998.

Raeder, J., Y. L. Wang, T. J. Fuller-Rowell, and H. J. Singer, Global simulation of magnetospheric space weather effects of the Bastille Day storm, *Sol. Phys.*, in press, 2002.

Rassbach, M. E., R. A. Wolf, and R. E. Daniell Jr., Convection in a Martian magnetosphere, *J. Geophys. Res.*, *79*, 1125–1127, 1974.

Reiff, P. H., and J. G. Luhmann, Solar wind control of the polar-cap voltage, in *Solar Wind-Magnetosphere Coupling*, edited by Y. Kamide and J. A. Slavin, pp. 453–476, Terra Sci., Tokyo, 1986.

Russell, C. T., G. Lu, and J. G. Luhmann, Lessons from the ring current injection during the September 24, 25, 1998 storm, *Geophys. Res. Lett.*, *27*, 1371–1374, 2000.

Siscoe, G. L., Towards a comparative theory of magnetospheres, in *Solar System Plasma Physics*, vol. 11, edited by C. F. Kennel, L. J. Lanzerotti, and E. N. Parker, pp. 299–402, North-Holland, New York, 1979.

Siscoe, G. L., N. U. Crooker, G. M. Erickson, B. U. Ö Sonnerup, K. D. Siebert, D. R. Weimer, W. W. White, and N. C. Maynard, Global geometry of magnetospheric currents, in *Magnetospheric Current Systems, Geophys. Monogr. Ser.*, vol. 118, edited by S.-I. Ohtani et al., pp. 41–52, AGU, Washington, D.C., 2000.

Smythe, W. R., *Static and Dynamic Electricity*, McGraw-Hill, New York, 1950.

Spreiter, J. R., A. L. Summers, and A. Y. Alksne, Hydromagnetic flow around the magnetosphere, *Planet. Space Sci.*, *14*, 223–253, 1966.

Tanaka, T., Generation mechanisms for magnetosphere-ionosphere current systems deduced from a three-dimensional MHD simulation of the solar wind-magnetosphere-ionosphere coupling process, *J. Geophys. Res.*, *100*, 12,057–12,074, 1995.

Tanaka, T., Field-aligned-current systems in the numerically simulated magnetosphere, in *Magnetospheric Current Systems*, edited by S.-I. Ohtani et al., *Geophys. Monogr. Ser.*, vol. 118, pp. 53–59, AGU, Washington, D.C., 2000.

Vasyliunas, V. M., J. R. Kan, G. L. Siscoe, and S.-I. Akasofu, Scaling relations governing magnetospheric energy transfer, *Planet Space Sci.*, *30*, 359–365, 1982.

White, W. W., J. A. Schoendorf, K. D. Siebert, N. C. Maynard, D. R. Weimer, G. L. Wilson, B. U. Ö. Sonnerup, G. L. Siscoe, and G. M. Erickson, MHD simulation of magnetospheric transport at the mesoscale, in *Space Weather, Geophys. Monogr. Ser.*, vol. 125, edited by P. Song, H. J. Singer, and G. L. Siscoe, pp. 229–240, AGU, Washington, D.C., 2001.

G. M. Erickson and G. L. Siscoe, Center for Space Physics, Boston University, Boston, MA 02215, USA. (siscoe@bu.edu)

N. C. Maynard, J. A. Schoendorf, K. D. Siebert, D. R. Weimer, W. W. White, and G. R. Wilson, Mission Research Corporation, Nashua, NH 03062, USA.

B. U. Ö. Sonnerup, Thayer School of Engineering, Dartmouth College, Hanover, NH 03755, USA.